DETERMINATION OF THE EFFECTIVE WATER CONDUCTIVITY OF SUGAR MAPLE SAPWOOD AND WHITE SPRUCE HEARTWOOD UNDER VACUUM

Maurice Defo
Graduate Student

Yves Fortin†
Professor

and

Alain Cloutier†
Assistant Professor

Département des sciences du bois et de la forêt
Faculté de foresterie et de géomatique
Université Laval
Québec. Qc
Canada G1K 7P4

(Received August 1998)

ABSTRACT

A macroscopic approach based on the water potential concept is proposed to represent the movement of water in wood during continuous vacuum drying. In order to solve the flow equation, the effective water conductivity under vacuum must be known. A new apparatus is proposed to determine this moisture transport coefficient based on the instantaneous profile method, where moisture content profiles are established at different drying times, making possible the measurement of the moisture flux and driving force at a given position. One-dimensional moisture flow measurements were conducted through two sides of a cubic wood specimen under constant temperature and absolute pressure. The effective water conductivity function was established from green to dry conditions at 60°C in the radial and tangential directions; at 8, 13, and 18 kPa for sugar maple sapwood; and at 8 kPa for white spruce heartwood. The results show that the effective water conductivity decreases exponentially from green conditions to about 35% moisture content for sugar maple. Beyond this point, the effective water conductivity decreases more gradually with a decrease in moisture content for both sugar maple and white spruce. The effective water conductivity is generally higher in radial than in tangential direction for both species. The results obtained for sugar maple show that the effective water conductivity increases significantly as the pressure decreases. The effect of pressure can be explained by the contribution of the apparent gas permeability. The contribution of the pressure potential to the total water potential can be neglected below fiber saturation point. The flux-gradient relationships obtained at given moisture contents are linear, confirming the validity of the flow equation based on water potential used in the present work.

Keywords: Water potential, effective water conductivity, vacuum drying, instantaneous profile method, sugar maple, white spruce.

INTRODUCTION

Wood drying is an essential requirement for the production of high quality construction lumber and secondary wood processing. Numerous drying techniques have been developed, among which is vacuum drying. During the last two decades, many studies have been devoted to vacuum drying of wood. Its main attraction is the reduction of the boiling point

† Member of SWST.

Wood and Fiber Science, 31(4), 1999, pp. 343–359

of water under partial vacuum. Therefore, free water can be vaporized and removed at temperatures below 100°C almost as rapidly as for high-temperature drying. Thus, thick, refractory, and high-value species can be safely dried in a vacuum kiln in a fraction of the time required in a conventional kiln. However, the drying schedules developed so far for vacuum drying rely mainly on empirical knowledge. One way to achieve the optimal control of wood drying under vacuum is mathematical modeling based on a physical description of heat and mass transfer inside wood. A few studies have been published in this respect (Moyne and Martin 1982; Fohr et al. 1995; Perré and Mosnier 1995; Guilmain et al. 1996; Sébastian et al. 1996; Audebert et al. 1997; Jomaa and Baixeras 1997).

BACKGROUND

A particular problem occurring when defining a model of moisture movement in wood during drying is the choice of the driving force. Different potentials are advocated in the literature. Following Babbit (1950), the use of a thermodynamic potential function characterizing the free energy status of water in wood has gained a wider acceptance during the last twenty years. The functions used are either the gradient in chemical potential (Kawai et al. 1978; Siau 1983, 1992; Skaar and Kuroda 1985; Stanish et al. 1986; Skaar 1988) or the gradient in water potential (Fortin 1979; Siau 1984; Cloutier et al. 1992; Cloutier and Fortin 1994). In the multi-component model proposed by Whitaker (1977), different driving forces are used, depending on the state of water in wood. For water in the liquid, gaseous, and bound states, driving forces are, respectively, the gradient in the pressure within the liquid, the gradient in total pressure, and the gradient in moisture content or in chemical potential (Stanish et al. 1986; Pang 1996; Perré 1987, 1996; Perré and Maillet 1989; Perré and Degiovanni 1990; Ouelhazi et al. 1992; Melaaen 1996).

The application of the water potential concept to the prediction of water movement in wood during drying has been described in detail by Fortin (1979). The water potential, ψ, is derived from classical thermodynamics as the difference between the specific Gibbs free energy of water in the state under consideration, and the specific Gibbs free energy of water in the standard reference state. The water potential is expressed in terms of energy per unit mass of water (J kg^{-1}) or its pressure equivalent (Pa). It may be thought of as the sum of the separate contributions of the various force fields acting on the water in wood. In the case of isothermal wood drying at atmospheric pressure, it has been demonstrated that the only significant component of water potential is the matric potential ψ_m (Fortin 1979; Cloutier and Fortin 1993). During vacuum drying, there is a significant bulk flow induced by a gradient in the total pressure (Moyne and Martin 1982). Thus, the pressure component ψ_p must be taken into account in the total water potential as follow:

$$\psi = \psi_m + \psi_p \quad (1)$$

Each of these components can be derived separately in terms of measurable parameters (Cloutier and Fortin 1991). At high moisture contents, ψ_m can be described by the following relation:

$$\psi_m = -\bar{V}_w P_m \quad (2)$$

where ψ_m = matric potential due to the combined effect of the capillary and sorptive forces; $\bar{V}_w$ = specific volume of water (m^3_{water} kg^{-1}_{water}); and P_m = equivalent matric pressure counterbalancing the effect of the capillary and sorptive forces due to the wood matrix (Pa). The component ψ_p is defined by the following relation:

$$\psi_p = \bar{V}_w P_e \quad (3)$$

where ψ_p = pressure potential describing the effect of a system bulk pressure either greater or less than the reference bulk pressure which by convention is taken as zero; P_e is the external hydrostatic or gas pressure (Pa).

Under the assumption of negligible temper-

ature gradients, the general expression for unsteady-state moisture movement in wood is given by the following relation (Cloutier and Fortin 1993):

$$\frac{\partial C}{\partial t} - \vec{\nabla} \cdot (\underline{\underline{K}}(M, T) \cdot \vec{\nabla}\psi) = 0 \qquad (4)$$

where C = moisture concentration (kg_{water} $m^{-3}{}_{moist\ wood}$); t = time (s); $\underline{\underline{K}}(M, T)$ = effective water conductivity tensor ($kg^2{}_{water}$ $m^{-1}{}_{moist\ wood}$ s^{-1} J^{-1}) (function of moisture content and temperature); and $\vec{\nabla}\psi$ = gradient in water potential (J $kg^{-1}{}_{water}$ $m^{-1}{}_{moist\ wood}$). In nonisothermal conditions, a term for moisture flow induced by the temperature gradient could be added.

The water potential approach is advantageous because it can be theoretically applied to water in wood in the three states (liquid water, water vapor, and bound water). Thus, a limited number of parameters are needed to solve the equation of mass transfer in wood during the drying process, namely, the moisture content-water potential relationship and the effective water conductivity of wood.

The "effective water conductivity," as used by Fortin (1979), Cloutier and Fortin (1993), and Tremblay et al. (1998), is a general term covering the processes of diffusion and mass flow. The water conductivity is qualified as "effective" because it takes into account all the flow mechanisms at work. Thus, the driving force is represented by only one potential gradient, which in this case is the water potential gradient. Near full saturation, it is equivalent to permeability. The scope of this study is limited to unsaturated conductivity. Different methods for predicting or measuring the unsaturated conductivity were described by Fortin (1979) and Cloutier and Fortin (1993). Among these methods, the instantaneous profile method allows the direct measurement of the effective water conductivity. The moisture content profiles are established at different drying times, allowing the evaluation of the flux of moisture and the driving force at a given position. This method presents two main advantages: 1) no specific set of boundary conditions is required, except that the flux must be known at one position; 2) the flux-gradient proportionality can be verified directly.

The instantaneous profile method has been used by Kawaï et al. (1978), Fortin (1979), Cloutier and Fortin (1993), and Tremblay et al. (1998). These studies have shown that the effective water conductivity is higher in absorption than in desorption, that it increases exponentially with moisture content and temperature, and that it is higher in radial direction than in tangential direction. The hysteretic behavior of the K(M) function is attributed to the "ink-bottle effect" as for the moisture content-water potential relationship (Fortin 1979). The variation of the moisture content-water potential relationship with temperature would explain a large part of the effect of temperature on K(M) (Cloutier and Fortin 1993).

To our knowledge, the literature shows no data with respect to the effect of pressure on the effective water conductivity. The separate flow mechanism approach may be used to assess this effect. According to the multi-component approach, the liquid flux takes place in wood under the influence of the pressure gradient in the liquid phase following Darcy's law (Perré et al. 1995):

$$\vec{q}_l = -\rho_l \frac{\underline{\underline{k}}\,\underline{\underline{k}}_{rl}}{\mu_l} \vec{\nabla} P_l \qquad (5)$$

where $\vec{q}_l$ = mass flux of the liquid phase (kg_l m^2 s^{-1}); ρ_l = density of the liquid (kg_l m_l^{-3}); $\underline{\underline{k}}$ = intrinsic permeability tensor (m^2); $\underline{\underline{k}}_{rl}$ = relative permeability tensor of the liquid phase (dimensionless); μ_l = dynamic viscosity of the liquid (Pa s); and $\vec{\nabla} P_l$ = pressure gradient in the liquid (Pa). The effect of pressure on the solid phase (wood matrix) can be assumed negligible (Perré et al. 1995). At 50°C, the density of water varies only by 4.4×10^{-5}% kPa^{-1} (Lide 1994/1995) and the viscosity as little as 0.04% when pressure changes from 100 kPa to 1,000 kPa (Sengers and Watson 1986). The intrinsic permeability, k, is a function of the porosity and the tortuosity of the

porous medium (Siau 1995; Perré et al. 1995). Since the pressure has no effect on the solid phase, k remains unchanged whatever liquid is considered. The relative permeability, k_{rl}, is a function of the degree of saturation only (Whitaker and Chou 1983; Perré et al. 1995). From the foregoing, the vacuum should therefore have no theoretical effect on the global transport coefficient of the liquid phase.

The mass flux of gas phase (water vapor) can be described as follows:

$$\vec{q}_v = -\rho_v \frac{\underline{\underline{k}}_g \underline{\underline{k}}_{rg}}{\mu_g} \vec{\nabla} P_g \qquad (6)$$

where $\vec{q}_v$ = mass flux of the water vapor ($kg_v\ m^{-2}s^{-1}$); ρ_v = density of the water vapor ($kg_v\ m_v^{-3}$); $\underline{\underline{k}}_g$ = apparent gas permeability tensor (m^2); $\underline{\underline{k}}_{rg}$ = relative permeability tensor of the gas phase (dimensionless); μ_g = dynamic viscosity of the gas phase (Pa s); and $\vec{\nabla} P_g$ = pressure gradient in the gas phase (Pa). Vapor pressure and density are related by the ideal gas law:

$$\rho_v = \frac{M_w P_v}{RT} \qquad (7)$$

where M_w = molecular weight of water (18.053×10^{-3} kg mol^{-1}); R = gas constant (8.3143 J mol^{-1} K^{-1}); P_v = partial pressure of the water vapor (Pa); and T = temperature (K). It is well known that in a capillary whose diameter is in the same order of magnitude as the molecular mean free path, Knudsen diffusion or slip flow occurs, resulting from collisions with the walls of the capillary (Siau 1995). From the kinetic theory of gases, the molecular mean free path increases with pressure reduction (Siau 1995). Thus, the probability for one particle to collide with the pore wall increases. Slip flow becomes predominant and the apparent gas permeability can be described by (Siau 1995):

$$k_g = k\left(1 + \frac{b}{\bar{P}_g}\right) \qquad (8)$$

where k_g = apparent gas permeability; k = intrinsic permeability; b = constant proportional to molecular mean free path and inversely proportional to pore radius (Pa); $\bar{P}_g$ = mean gas pressure (Pa). Due to slip flow, the apparent gas permeability increases significantly as the pressure decreases in wood. It can double when the pressure drops from 100 kPa to 50 kPa (Perré 1987). Therefore, if one substitutes Eqs. (7) and (8) into Eq. (6), and takes into account the negligible effect of pressure on both the partial pressure of water vapor (Edlefsen and Anderson 1943) and the viscosity of gases (Sengers and Watson 1986), one could expect an increase of the effective permeability of the gas phase with a decrease of pressure.

In the hygroscopic range, the flow mechanism involved is mainly diffusion, including diffusion of bound water in the cell walls and diffusion of water vapor in the lumens. The effect of pressure on the bound water properties can be assumed negligible (Perré et al. 1995). From the kinetic theory of gases, Perré et al. (1995) have shown that the effective vapor diffusivity increases when the pressure decreases. Świgoń (1993) and Świgoń and Kurasiak (1995) also reported an increase of the diffusion coefficient with a decrease in pressure:

$$D = D_N\left(\frac{T}{T_N}\right)^{1.82}\frac{P_N}{P} \qquad (9)$$

where D = diffusion coefficient ($m^2\ s^{-1}$) at a given pressure P below atmospheric pressure P_N (Pa); D_N = diffusion coefficient at atmospheric pressure ($m^2\ s^{-1}$); T = temperature (K); and T_N = normal temperature (273 K). Because of slip flow and the increase of water vapor diffusivity at reduced pressures, one can expect an increase of the effective water conductivity under vacuum since it incorporates all these transport coefficients.

The objectives of this work were: 1) to develop an apparatus for the determination of the effective water conductivity of wood under vacuum assuming that the moisture content-water potential relationship is known; 2) to measure the effective water conductivity of

sugar maple (*Acer saccharum* Marsh.) sapwood and white spruce (*Picea glauca* (Moench.) Voss.) heartwood, from green to dry conditions. The effective water conductivity function determined in this study will be used to model mass transfer in wood during vacuum drying. The effect of pressure on the effective water conductivity of wood is also assessed.

MATERIAL AND METHODS

Material

The material used for this study was obtained from a natural stand located in the southeast part of Québec, Canada. The trees, six for each species, were felled in the late fall in the case of sugar maple and in the early winter in the case of spruce. The age of the trees varied from 65 to 121 and from 81 to 100 years at DBH for sugar maple and white spruce, respectively. Depending on the diameter of the tree, three to four 1.22 m-long-bolts were cut from the stem. The specimens used for this study were randomly selected from the second, third, and fourth (if necessary) bolts. They were 45 × 45 × 45 mm (L × R × T) in dimension and free of visual defects. They were all sapwood in the case of sugar maple and all heartwood in the case of spruce. Depending on the initial moisture content and the target pressure level, four to eight groups for each combination of direction of flow and pressure were formed. Each group was composed of eight specimens. Six specimens were used for the determination of the moisture content profiles and the two remaining specimens for temperature and pressure measurements. After selection and classification, the specimens were kept in sealed polyethylene bags and stored at −15°C prior to their use in the experiments. Before each experiment, the specimens were kept over distilled water for 24 h in a closed desiccator at 21°C to allow them to thaw.

The specific gravity (oven-dry weight/green volume) of the sugar maple specimens considered in this study varied from 0.587 to 0.676 with an average initial moisture content of about 60%. For white spruce specimens, the specific gravity varied from 0.318 to 0.427 with an average initial moisture content of about 35%.

Experimental apparatus

A new apparatus was designed to determine the effective water conductivity under vacuum. One-dimensional moisture flow measurements were then conducted through two sides of a cubic specimen under constant temperature and absolute pressure. The main part of the apparatus (Fig. 1) consisted in two 1.5-m-long manifolds mounted on a stand. Eight pairs of 12.7-mm-thick grooved metal plates connected to the feed and collector manifolds were used to heat the test specimens. Interconnected channels have been drilled inside the plates to allow the circulation of hot water. Each pair of metal plates was held together by two metal rods with coil springs at one end to ensure that the plates remain in close contact with the specimen, even in the case of an important shrinkage. This ascertained heat transfer efficiency from the plates to the wood specimen. A thermostatic water bath provided the hot water to the eight units placed inside a small laboratory vacuum kiln (diameter = 0.4 m; length = 2.2 m).

The main difficulty with the apparatus was to adjust the rate of hot water flow inside the contact plates. This was controlled by individual valves as illustrated in Fig. 1. By adjusting these valves, it was possible to maintain the 16 plates within ±1°C.

Methods

The specimens were edge-coated with a silicone sealant and aluminum foil, and insulated with styrofoam. The open faces of the specimens were then put in contact with the heating plates. One specimen was used to measure the local temperatures in wood with copper-constantan thermocouples and another one was used to measure local pressures in wood using 1.2-mm-diameter stainless steel tubes con-

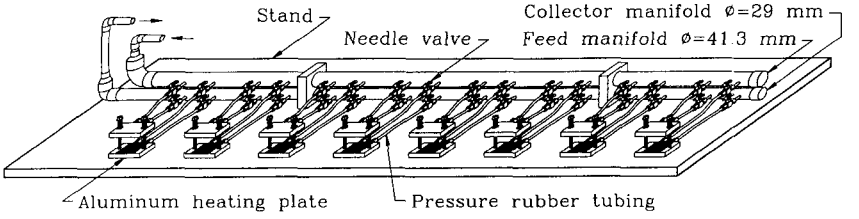

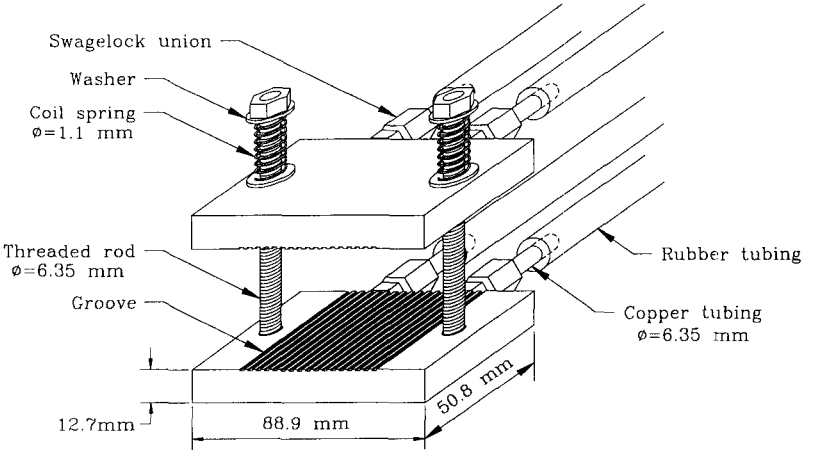

FIG. 1. Experimental apparatus.

nected to pressure sensors. The temperature and pressure measurements were taken at 1.0, 11.25, and 22.5 mm from one drying surface. All temperatures and pressures were recorded with a Strawberry Tree data acquisition board and software (Quicklog) installed in a 386 PC. The digital on/off control feature of the data acquisition board was used to maintain the vacuum kiln ambient pressure within ±0.2 kPa.

When all the specimens and sensors were in place, the setup was enclosed inside the vacuum kiln. The temperature of the water circulating in the manifold was 65°C and was kept constant by the water bath. The specimens were heated at atmospheric pressure and 100% RH until the wood core temperature reached the target value (60°C) after 2 h. Air circulation during the heating phase was achieved by 11 small fans (diameter = 0.14 m) at the bottom of the cylinder, which produced an air velocity of about 2.5 m s^{-1}. Humidification was performed with low pressure steam (10 kPa) and was controlled by the dry and wet bulb temperatures. Then, the vacuum phase followed until the end of the drying process. Vacuum was produced by a liquid-ring pump capable of reducing the pressure down to 5 kPa.

One absolute pressure level (8 kPa) was considered for white spruce and three pressure levels for sugar maple (8, 13, and 18 kPa). The effective water conductivity was measured in the radial and tangential directions for both species. For a given combination of direction of flow and pressure level, a separate drying

run was performed for each moisture content profile measured. This was to avoid hysteresis and back flow effects that would have occurred in a one-step drying run where a group is removed from time to time for a moisture content profile determination. The drying time required for each run was established during preliminary tests. Drying times of sugar maple test specimens from an average initial MC of 60% to 7% were 10, 17, and 60 h at 8, 13, and 18 kPa, respectively; whereas the spruce test specimens dried from 35% to 7% average MC in 10 h at 8 kPa absolute pressure.

We did not measure the actual relative humidity inside the cylinder during drying, but the surface moisture contents obtained at the end of each drying run indicated that it was much lower than the expected theoretical values (total pressure inside the cylinder/saturated vapor pressure at dry bulb temperature). One explanation for this discrepancy is that it is likely that air never vanishes completely from the cylinder, despite the pressure reduction; thus, the water vapor pressure inside the cylinder is lower than the total pressure. Also, the vacuum cylinder was not perfectly sealed and allowed some air infiltration. However, it should be noted that the boundary conditions have no effect on the effective water conductivity calculated with the instantaneous profile method since the water flux and the gradient of water potential are both measured in the specimens.

At the end of each drying run, six of the eight specimens were cut in the flow direction into 11 slices (each slice having nearly 3.5 mm in thickness) using a thin kerf band saw (0.5-mm kerf). The mass and volume of each slice were quickly measured to avoid moisture loss. The slices were then dried at 105°C until constant weight in order to determine their moisture content and then, their moisture concentration.

Equation (4) was used in order to determine the effective water conductivity. If the chosen coordinates system coincides with the principal directions of the tensor and of wood, $\underline{\underline{K}}(M, T)$ is diagonal and its components correspond to its eigenvalues. In this case, the expression for one-dimensional isothermal moisture movement is:

$$\frac{\partial C}{\partial t} - \frac{\partial}{\partial x}\left[K_x(M, T)\frac{\partial \psi}{\partial x}\right] = 0 \qquad (10)$$

where $K_x(M, T)$ is the unsaturated effective water conductivity, a function of moisture content and temperature; and $\partial\psi/\partial x$ is the water potential gradient in the x direction.

The relationship between wood moisture content and water potential was established for sugar maple sapwood and for white spruce heartwood from green to dry conditions in a previous study (Defo et al. 1998), for material of the same origin as that used in the present work. The pressure component, ψ_p, was calculated from Eq. (3) with pressure values measured at different positions inside the specimens during the experiments.

The equation actually used to determine the effective water conductivity is obtained by differentiation and integration of Eq. (10) (Cloutier and Fortin 1993):

$$K_x(M, T)_{x_i,t_j} = \frac{\dfrac{\partial}{\partial t}\displaystyle\int_{x_{q=0}}^{x_i} C\, dx}{\left[\dfrac{\partial \psi}{\partial x}\right]_{x_i,t_j}} = \frac{\left[\dfrac{\partial I}{\partial t}\right]_{x_i,t_j}}{\left[\dfrac{\partial \psi}{\partial x}\right]_{x_i,t_j}} \qquad (11)$$

where $K_x(M, T)_{xi,tj}$ = effective water conductivity in the direction of flow x at position x_i and time t_j, $[\partial I/\partial t]_{xi,tj}$ = flux through the plane x_i at time t_j; and $[\partial\psi/\partial x]_{xi,tj}$ = water potential gradient at x_i and t_j.

The boundary conditions were the same for the two faces of the specimen in contact with the heating plates. The problem was then symmetric about the plane $x_{q=0}$, which was the middle plane of the specimen (x = 22.5 mm), perpendicular to the flow direction. Therefore, only one half of the cross section was considered for computations.

The average moisture concentration profiles were fitted to the data points using a software called "Table Curve," each data point representing the average moisture concentration at

a given position for the six specimens of a group and the two corresponding positions located each side of the middle plane. The integral I at t_j was determined by the integration of the area defined by the average moisture concentration profile at t_j and the planes x_i and $x_q = 0$. The term $[\partial I/\partial t]_{xi,tj}$ was determined by plotting I against t and calculating the slope at t_j. The water potential gradient $[\partial\psi/\partial x]_{xi,tj}$ was obtained following two steps: 1) the value of ψ_m at position x_i and time t_j was inferred from the M-ψ relationship determined by Defo et al. (1998). The effect of temperature was considered in the determination of ψ_m; 2) the ψ_p value at x_i and t_j were calculated using Eq. (3) and measured pressure values, and then added to the corresponding ψ_m values to obtain the total ψ values. The ψ profile at t_j was plotted and the ψ gradient at x_i was determined by calculating the slope. The effective water conductivity was determined using Eq. (11) for seven different positions: 24, 27, 30, 33, 36, 39, and 42 mm, corresponding to 1.5, 4.5, 7.5, 10.5, 13.5, 16.5, and 19.5 mm from the position $x_{q\ 0}$.

RESULTS AND DISCUSSION

Effective water conductivity-moisture content relationship

The effective water conductivity-moisture content relationships obtained for sugar maple sapwood are shown in Figs. 2 and 3 for the radial and tangential directions, respectively. The effective water conductivity-moisture content relationships obtained for white spruce heartwood are presented in Fig. 4 for the radial and tangential directions. Each position considered for computation is represented by a distinctive symbol. The curves were hand fitted to the data points. The relative superposition of the data points as shown in Figs. 2 to 4 indicates that, for any given moisture content, the effective water conductivity determined by the instantaneous profile method has a unique value, independent of the position.

As shown in Figs. 2 and 3, the effective water conductivity of sugar maple decreases

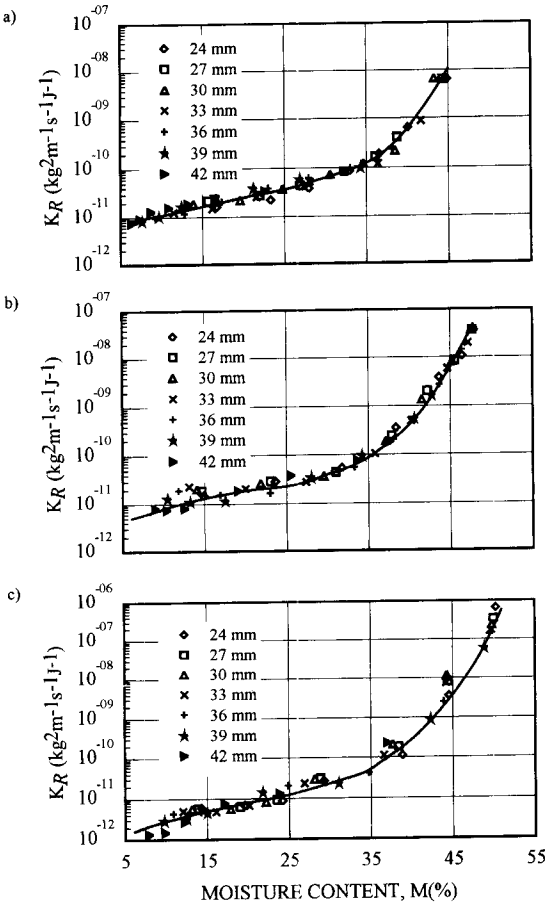

FIG. 2. Effective water conductivity of sugar maple sapwood in the radial direction (K_R) at 60°C. a) 8 kPa; b) 13 kPa; c) 18 kPa.

abruptly from the green condition to about 35% M. Below 35% M, the effective water conductivity of both sugar maple and white spruce (Figs. 2 to 4) decreases more gradually with a change in moisture content. The steep decrease of the effective water conductivity from the green condition to 35% M may be due to simultaneous liquid and water vapor flow resulting from a large gas pressure difference (Moyne and Martin 1982; Perré et al. 1995; Chen and Lamb 1995). In the later stage of drying (below 35% M), moisture movement would occur by a diffusion process but, as will be discussed later, it is likely that a hydrodynamic flow of water vapor is also present. The

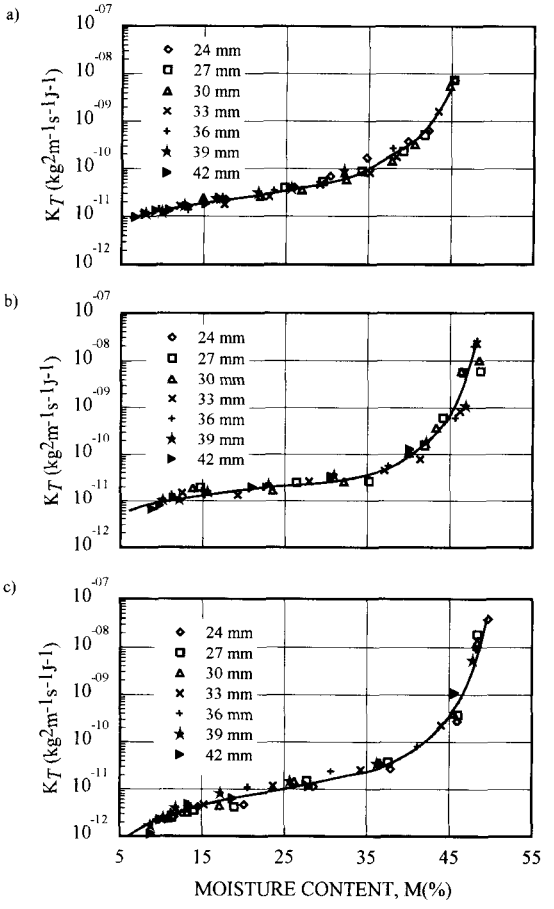

FIG. 3. Effective water conductivity of sugar maple sapwood in the tangential direction (K_T) at 60°C. a) 8 kPa; b) 13 kPa; c) 18 kPa.

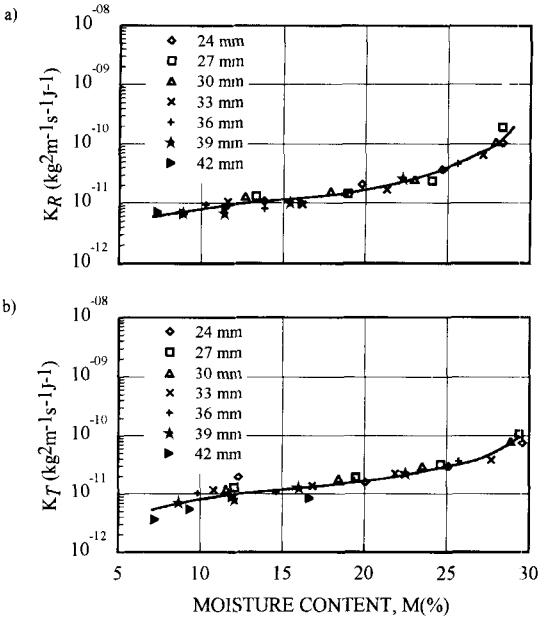

FIG. 4. Effective water conductivity of white spruce heartwood at 60°C and 8 kPa. a) radial direction (K_R); b) tangential direction (K_T).

inflexion point of the effective water conductivity curve would correspond to the moisture content level at which the liquid phase continuity is disrupted and the liquid flow caused by capillary effects is no longer possible.

The effective water conductivity varies also with the structural direction of wood as depicted in Table 1. At a given pressure and for moisture contents above 20% M, K_R is higher than K_T. The K_R/K_T ratio varies from 1.1 to 10.3 at 18 kPa; 1.0 to 8.3 at 13 kPa; and 1.0 to 2.4 at 8 kPa. Below 20% M, the K_R/K_T ratio is close to unity. The maximum possible error yielded by the instantaneous profile method has been previously evaluated to vary from ±20% to ±45% of the K-value (Cloutier and Fortin 1993), which is small when considering the fact that the K-values cover a range of several orders of magnitude. With the uncertainty associated to the curves, we cannot conclude to any marked differences between K_R and K_T at low M values. A similar observation has also been reported by Cloutier and Fortin (1993) for aspen sapwood dried at atmospheric pressure. These authors concluded that the high values of K_R at M above 20% would indicate the contribution of wood rays to the bulk flow. At low moisture contents, the flow is of diffusive type. Thus, the contribution of wood rays on K_R would be smaller at low M values than at high M values. It should be noted that for a given moisture content, the ratio K_R/K_T at high M values at 18 kPa is higher than the K_R/K_T ratio at 13 kPa, which in turn is higher than K_R/K_T ratio at 8 kPa. This variation of the K_R/K_T ratio with pressure may be attributed to the change of the mass-transfer mechanism with pressure reduction.

TABLE 1. *Variation of the K_R/K_T ratio with pressure and moisture content.*

Species	M (%)	Pressure (kPa) 8	13	18
	7	0.9	0.8	1.4
	9	0.9	0.9	1.3
	11	0.9	0.9	1.2
	13	0.9	0.9	1.1
	15	0.9	1.0	1.1
	17	0.9	1.0	1.1
	19	1.0	1.0	1.1
	21	1.0	1.1	1.2
	23	1.1	1.1	1.2
	25	1.1	1.2	1.2
	27	1.1	1.3	1.3
Sugar maple	29	1.2	1.4	1.4
	31	1.3	1.6	1.5
	33	1.3	1.9	1.8
	35	1.3	2.3	2.2
	37	1.3	3.0	2.9
	39	1.5	4.1	4.1
	41	2.2	5.6	6.0
	43	2.4	7.3	8.4
	45	2.2	8.3	10.3
	7	1.1		
	9	1.0		
	11	1.0		
	13	1.0		
	15	1.0		
White spruce	17	1.0		
	19	1.0		
	21	1.0		
	23	1.2		
	25	1.4		
	27	1.8		
	29	2.4		

Effect of pressure on the effective water conductivity

There are no available data on the effective water conductivity of sugar maple and white spruce at atmospheric pressure. The radial and tangential boundary desorption curves of the effective water conductivity functions of aspen sapwood established at atmospheric pressure and at 50°C by Cloutier and Fortin (1993) were used for comparison purposes. Only the K_R and K_T values between 10 and 70% were considered. These curves, together with the curves of the effective water conductivity of sugar maple sapwood at 18 kPa, are shown in Fig. 5. It appears that the K_R and K_T curves for sugar maple under vacuum are different in shape than those of aspen sapwood at atmospheric pressure. From Figs. 2 and 3, it is obvious that pressure has an effect on the effective water conductivity. To clearly illustrate this phenomenon, the effective water conductivity of sugar maple was plotted against absolute pressure at different M values as shown in Fig. 6. At a given M, the effective water conductivity increases as the absolute pressure decreases, both in the radial and tangential directions. At high M values, the effective water conductivity incorporates the liquid and the vapor fluxes. The high values of the effective water conductivity observed at high moisture contents can be explained by the contribution of the apparent gas permeability which increases with a reduction of the ambient pressure as predicted by Eq. (8). On the other hand, when wood is dried below FSP, the air can leave the lumina, and diffusion becomes more efficient as there are fewer air molecules hindering the free movement of water vapor molecules (Neumann et al. 1992). As predicted by Eq. (9), the effective water conductivity at 10 and 20% M (Fig. 6) tends to be inversely proportional to the absolute pressure.

Flow mechanisms

Numerous studies assumed that the faster drying observed under vacuum may be attributed to the boiling phenomenon. Figure 7 shows the pressure levels measured in the specimen of sugar maple sapwood at different depths during radial vacuum drying at 8 kPa. The saturated vapor pressures (P_{vs}) corresponding to the local temperatures are also shown in Fig. 7. It is clear that boiling does not occur inside wood since pressures measured inside the specimens are always higher than the saturated vapor pressures, except for the few millimeters below the surface and at the end of the drying (M = 6%) where the measured pressures are lower than the saturated vapor pressures. This observation was also made by Neumann et al. (1992) and Chen and Lamb (1995). As shown in Fig. 7 and as point-

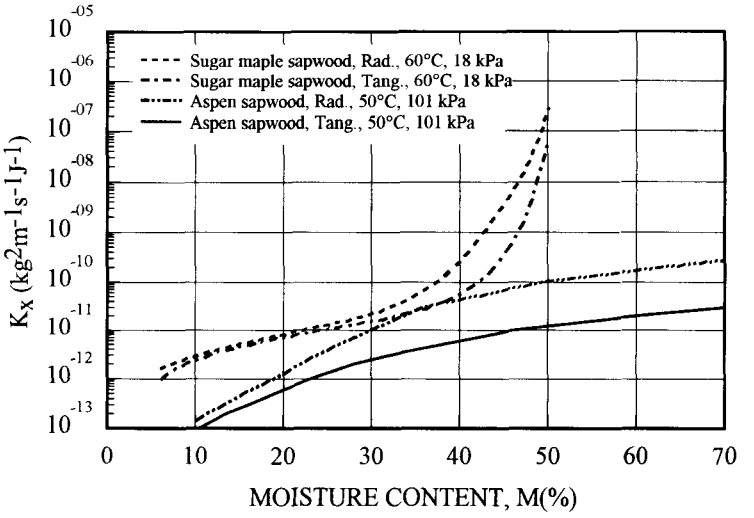

FIG. 5. Effective water conductivity of sugar maple sapwood at 60°C and 18 kPa and aspen sapwood at atmospheric pressure and 50°C (adapted from Cloutier and Fortin 1993).

ed out by Chen and Lamb (1995), there is a boiling front (region where P is less than or equal to P_{vs}) which retreats from the surface towards the center as the drying proceeds, the retreating velocity being a function of the heat supply and certain properties of wood, such as permeability, specific gravity, and conductivity (Chen and Lamb 1995). Thus, when the liquid phase continuity is not disrupted, moisture migrates from the center to the boiling front in the liquid phase and from the boiling front to the surface in the gas phase. When continuity is disrupted, moisture migrates essentially in the gas phase. It must be noticed that this scheme could be different in other vacuum drying technologies.

As previously mentioned, it is possible that below FSP water vapor also migrates under the influence of the total gas pressure gradients. Figure 7 shows that until the end of drying, there is a difference between the pressure in the center of the specimen and the ambient pressure. The intense evaporation taking place inside wood keeps the pressure up, whereas the surface pressure is maintained at the pressure of the chamber. This observation is somewhat analogous to the one made by Neumann et al. (1992). They calculated the diffusion coefficients based on Fick's first law from experimental data obtained for beech boards dried in a conventional kiln and in a convective vacuum kiln in superheated steam at 20 kPa. At low moisture contents, the diffusion coefficient obtained during vacuum drying was several times higher than during conventional drying. The authors concluded that Fick's law was not applicable to vacuum drying. Chen and Lamb (1995) reported that mass flow is the most important transport mechanism under vacuum rather than diffusion, which is dominant for conventional drying. Noack (1965) quoted by Chen and Lamb (1995) found that moisture migrates in the gas state when wood dries below FSP during vacuum drying. He concluded that the driving force was the pressure difference between the vapor pressure in the lumen and the ambient pressure. Using steam explosion to improve the permeability of wood, Hayashi et al. (1993, 1995) found that the drying rate obtained for radiofrequency/vacuum drying of the treated specimens was higher than for the control specimens in the whole range of moisture contents, confirming the impact of permeability on moisture movement below FSP. The transport coefficient for hydrodynamic

TABLE 2. *Summary of the regression analysis carried out for the flux-gradient relationships.*

Species	Direction	P kPa	M %	$q = q_0 + K_x Gr^*$ q_0 $\times 10^{-5}$ kg m^{-2}s^{-1}	K_x $\times 10^{-11}$ kg^{2}m^{-1}s^{-1}J^{-1}	S_{Kx} $\times 10^{-11}$ kg^{2}m^{-1}s^{-1}J^{-1}	R^2 %
			15	−1.91	2.26	0.29	95.3
Sugar maple	R	8	20	−0.85	3.15	0.22	97.6
			30	0.70	7.38	0.27	99.5
			40	1.02	28.09	2.87	98.0
			15	0.97	1.03	0.11	94.9
Sugar maple	R	13	20	0.12	1.88	0.19	95.2
			30	−0.92	5.30	0.39	97.3
			40	1.33	33.32	4.81	92.3
			15	0.02	0.49	0.02	99.2
Sugar maple	R	18	20	−0.20	1.02	0.07	97.4
			30	−0.30	3.77	0.71	84.8
			40	−0.47	39.97	13.72	62.9
			15	0.67	1.77	0.22	94.2
Sugar maple	T	8	20	0.04	2.62	0.28	95.6
			30	−0.22	5.68	0.76	93.4
			40	0.32	24.55	1.26	99.5
			15	0.15	1.46	0.07	98.8
Sugar maple	T	13	20	−0.24	1.89	0.09	98.8
			30	−0.72	3.33	0.15	98.9
			40	−1.48	11.42	1.88	88.1
			15	−0.10	0.57	0.05	96.0
Sugar maple	T	18	20	0.10	0.74	0.11	90.9
			30	0.20	1.75	0.13	97.5
			40	0.01	5.47	0.18	99.5
			15	0.76	0.85	0.08	95.9
White spruce	R	8	20	0.16	1.68	0.08	99.2
			25	0.10	3.11	0.29	97.5
			15	0.33	0.88	0.03	99.5
White spruce	T	8	20	−0.37	1.87	0.14	97.9
			25	−0.64	4.40	0.40	97.6

* $Gr = -(\partial\psi/\partial x)$.

oped for this purpose. The effective water conductivity was determined from green to dry conditions at 60°C in the radial and tangential directions; at 8, 13, and 18 kPa for sugar maple sapwood; and at 8 kPa for white spruce heartwood.

The effective water conductivity was found to decrease abruptly from the green condition to 35% moisture content. Beyond this point, the effective water conductivity decreased slowly with a decrease in moisture content. At a given pressure and for moisture contents above 20% M, K_R is higher than K_T. The K_R/K_T ratio varied from 1.1 to 10.5 at 18 kPa, 1.0 to 8.3 at 13 kPa, and 1.0 to 2.6 at 8 kPa. Below 20% M, the K_R/K_T ratio was close to unity. The effective water conductivity increased significantly as the pressure decreased. The effect of pressure can be explained by the contribution of the apparent gas permeability. It is likely that at moisture contents below FSP, water vapor migrates inside wood both by diffusion and under the influence of the total gas pressure gradient. The contribution of the pressure potential to the total potential was negligible at low moisture contents. The flux-

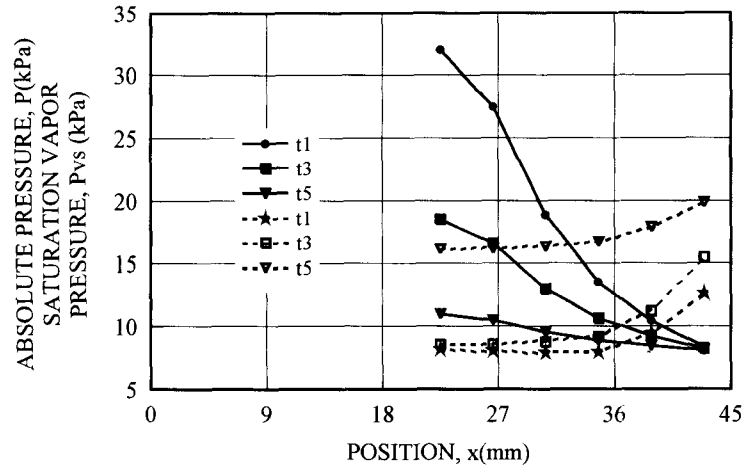

FIG. 7. Measured total pressures (solid lines) in sugar maple sapwood specimens during radial drying at 60°C and 8 kPa and saturated vapor pressures (dotted lines). t1) 74 min, M = 37%; t3) 197 min, M = 24%; t5) 631 min, M = 6%.

it reached the plate temperature. The maximum temperature difference between the surface and the center of the specimen was 3°C at 18 kPa, 6.2°C at 13 kPa, and 13.7°C at 8 kPa. With these large temperature gradients, especially at 8 kPa, the utilization of Eq. (4) may appear questionable since it does not show a thermal diffusion term explicitly. Therefore, it is necessary to check the flux-gradient relationship to verify the validity of Eq. (4) under our experimental conditions.

From Darcy's law, if the flux q is plotted against $-\partial\psi/\partial x$ at a given M, a straight line should be obtained with the slope corresponding to the effective water conductivity. The flux-gradient relationships were established at 15, 20, 30, and 40% M from the original data points obtained at the seven positions considered for computation of the effective water conductivity. The results of the regression lines fitted to the data points are presented in Table 2. Figure 9 shows the flux-gradient relationships obtained for sugar maple at 18 kPa in the radial direction and at 8 kPa in the tangential direction, which are respectively the worst (R^2 = 62.9) and the best (R^2 = 99.5) cases. The flux-gradient relationship was linear in all cases, with the intercept being randomly positive or negative. In most cases, the slopes of the regression line were in agreement, within $\pm S_{Kx}$, to the values obtained for K_R and K_T (Figs. 2, 3, and 4). These results show that, in spite of the nonisothermal drying, Darcy's law generalized to unsaturated flow holds, even under vacuum.

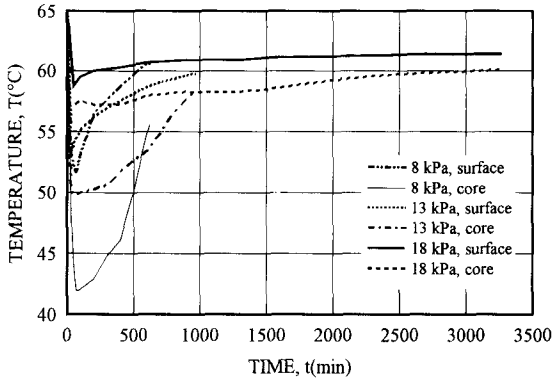

FIG. 8. Measured temperatures in sugar maple sap

CONCLUSIONS

The main objective of this study was to determine the effective water conductivity of wood under vacuum using the instantaneous

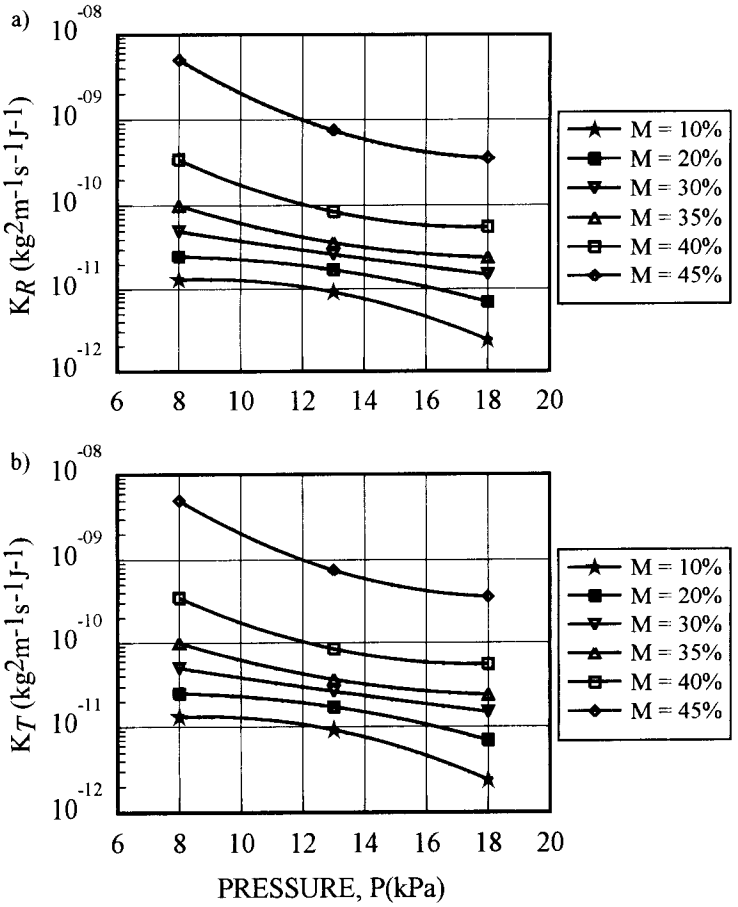

FIG. 6. Effective water conductivity of sugar maple sapwood as a function of absolute pressure. a) radial (K_R) direction; b) tangential (K_T) direction.

flow, k_g, is large compare to the one for diffusion. Therefore, it is easy to understand why the effective water conductivity under vacuum is greater than at atmospheric pressure.

Relative importance of the pressure potential

Equation (1) states that the total water potential is the sum of the separate contributions of the matric and pressure potentials. At 18 kPa, the contribution of ψ_p to the total potential ψ represents 0.31, 0.78, 22, and 24% for moisture contents of 12.8, 22.3, 38.1, and 49.8%, respectively. Thus, ψ_p must be taken into account above FSP whereas under FSP ψ_p can be neglected in the computation of the total potential.

Flux-gradient relationship

The determination of the effective water conductivity from Eq. (10) is based on the assumption of isothermal drying. However, it was very difficult to satisfy the isothermal condition for vacuum drying. Figure 8 shows changes in temperature inside the specimens during radial drying at 8, 13, and 18 kPa in the case of sugar maple. The temperature of the plate surface was maintained at 60 ± 2°C. When drying began, the temperature at the surface and inside the specimens dropped rapidly, indicating an intense evaporation without a sufficient heat supply to compensate for the latent heat of vaporization of water. As drying went on, the temperature rose gradually until

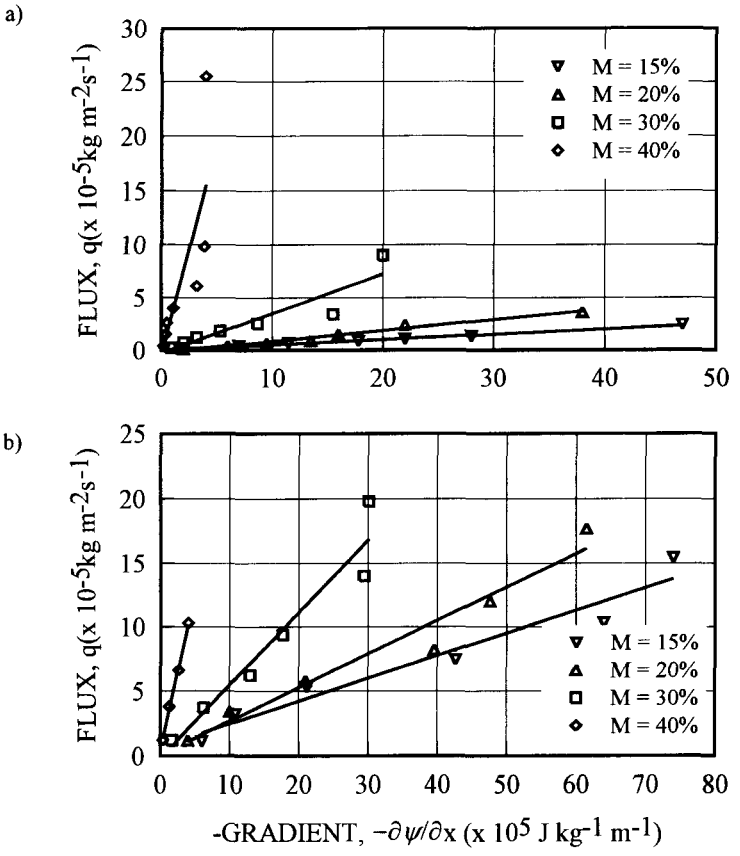

FIG. 9. Flux-gradient relationship obtained for sugar maple sapwood. a) radial direction, 18 kPa; b) tangential direction, 8 kPa.

gradient relationships obtained at given moisture contents were linear, confirming the validity of the flow equation based on water potential used in the present work. The results obtained will be used to model moisture movement in wood during continuous vacuum drying.

ACKNOWLEDGMENTS

This research project is supported by the Programme Pluriannuel des Bourses Canada-Cameroun, the Ministère des Ressources Naturelles du Québec, and by the Natural Sciences and Engineering Research Council of Canada under grant no. OGP0121954.

REFERENCES

AUDEBERT, P., A. TEMMAR, F. HAMMOUN, AND C. BASILICO. 1997. Vacuum drying of oak wood: Moisture, strains and drying process. Drying Technol. 15(9):2281–2302.

BABBIT, J. D. 1950. On the differential equations of diffusion. Can. J. Res. Sect. A. 28:449–474.

CHEN, Z., AND M. LAMB. 1995. The internal conditions in vacuum drying of wood. Pages 45–53 *in* P. Trebula, ed. Vacuum drying of wood '95. High Tatras, Slovak Republic.

CLOUTIER, A., AND Y. FORTIN. 1991. Moisture content-water potential relationship of wood from saturated to dry conditions. Wood Sci. Technol. 25:263–280.

———, AND ———. 1993. A model of moisture movement in wood based on the water potential and the determination of the effective water conductivity. Wood Sci. Technol. 27:95–114.

———, AND ———. 1994. Wood drying modelling based on the water potential concept: Hysteresis effect. Drying Technol. 12(8):1793–1814.

———, Y. FORTIN, AND G. DHATT. 1992. A wood drying finite element model based on the water potential concept. Drying Technol. 10(5):1151–1181.

DEFO, M., Y. FORTIN, AND A. CLOUTIER. 1998. Moisture content-water potential relationship of sugar maple and white spruce wood from green to dry conditions. Wood Fiber Sci. 31(1):62–70.

EDLEFSEN, N. E., AND A. B. C. ANDERSON. 1943. Thermodynamics of soil moisture. Hilgardia 15(2):31–298.

FOHR, J. P., A. CHAKIR, AND A. M. A. DU PEUTRY. 1995. Vacuum drying of oak wood. Drying Technol. 13(8&9): 1675–1693.

FORTIN, Y. 1979. Moisture-content matric potential relationship and water flow properties of wood at high moisture contents. Ph.D. thesis, University of British Columbia, Vancouver, BC. 187 pp.

GUILMAIN, C., O. BAIXERAS, AND W. JOMAA. 1996. Discontinuous and convective vacuum drying of oak: Experimental and modelling studies. Pages 147–158 *in* A. Cloutier, Y. Fortin, and R. Gosselin, eds. 5th International IUFRO Wood Drying Conference, Quebec City, Canada.

HAYASHI, K., Y. KANAGAWA, AND M. YASUJIMA. 1993. Change of dryability under vacuum drying by improvement of permeability of wood. Pages 112–118 *in* P. Trebula, ed. Vacuum drying of wood '93. High Tatras, Slovak Republic.

———, Y. NAGASE, AND Y. KANAGAWA. 1995. Experimental evidence of an importance of permeability in the RF/vacuum drying. Pages 261–269 *in* P. Trebula, ed. Vacuum drying of wood '95. High Tatras, Slovak Republic.

JOMAA, W., AND O. BAIXERAS. 1997. Discontinuous vacuum drying of oakwood: modelling and experimental investigations. Drying Technol. 15(9):2129–2144.

KAWAI, S., K. NAKATO, AND T. SADOH. 1978. Moisture movement in wood below the fiber saturation point. Mokuzai Gakkaishi 24(5):273–280.

LIDE, D. R. (ed.) 1994/1995. CRC Handbook of chemistry and physics, 75th. ed. CRC Press, Inc. Cleveland, OH.

MELAAEN, M. C. 1996. Numerical analysis of heat and mass transfer in drying and pyrolysis of porous media. Numerical Heat Transfer, Part A. 29:331–355.

MOYNE, C., AND M. MARTIN. 1982. Etude expérimentale du transfert simultané de chaleur et de masse au cours du séchage par contact sous vide d'un bois résineux. Int. J. Mass Transfer 25(12):1839–1848.

NEUMANN, R., A. MIELKE, AND G. BÖHNER. 1992. Comparison of conventional and convective vacuum drying of beech. Pages 222–226 *in* M. Vanek, ed. Proc. 3rd IUFRO International Wood Drying Conference, Vienna, Austria.

NOACK, D. 1965. Sonderverfahren der holztrocknung. Holzwirtschaftliches Jahrbuch No. 15, Holztrocknung. DRW-Verlags-Gm6H., Stuttgart, Germany.

OUELHAZI, N., G. ARNAUD, AND J. P. FOHR. 1992. A two dimensional study of wood plank drying. The effect of gaseous pressure below boiling point. Transport in Porous Media 7:39–61.

PANG, S. 1996. Moisture content gradient in a softwood board during drying: Simulation from 2-D model and measurement. Wood Sci. Technol. 30:165–178.

PERRÉ, P. 1987. Le séchage convectif des bois résineux. Choix, validation et utilisation d'un modèle. Thèse de Doctorat. Université de Paris VII, Paris, France. 251 pp.

———. 1996. The numerical modelling of physical and mechanical phenomena involved in wood drying: An excellent tool for assisting with the study of new processes. Tutorial. Pages 11–38 *in* A. Cloutier, Y. Fortin, and R. Gosselin, eds. 5th International IUFRO Wood Drying Conference, Quebec City, Canada.

———, AND D. MAILLET. 1989. Drying of softwood: The interest of a two dimensional model to simulate anisotropy or to predict degrade. Pages 226–237 *in* F. Kayilan, J. A. Johnson, and W. R. Smith, eds. Proc. IUFRO International Wood Drying Symposium. Seattle, WA.

———, AND A. DEGIOVANNI. 1990. Simulation par volumes finis des transferts couplés en milieux poreux anisotropes: Séchage du bois à basse et à haute température. Int. J. Heat Mass Transfer 33(11):2463–2478.

———, AND S. MOSNIER. 1995. Vacuum drying with radiative heating: Experiment on different species (fir, spruce and beech) and simulation with a simple analytical model. Pages 251–260 *in* P. Trebula, ed. Vacuum Drying of Wood '95, Zvolen, Slovak Republic.

———, P. JOYET, AND D. ALÉON. 1995. Vacuum drying: Physical requirements and practical solutions. Pages 7–34 *in* P. Trebula, ed. Vacuum Drying of Wood '95, Zvolen, Slovak Republic.

SÉBASTIAN, P., W. JOMAA, AND I. W. TURNER. 1996. A new model for the vacuum drying of wood based on the concept of the transition layer. Pages 191–205 *in* A. Cloutier, Y. Fortin, and R. Gosselin, eds. 5th International IUFRO Wood Drying Conference, Quebec City, Canada.

SENGERS J. W., AND J. T. R. WATSON. 1986. Improved international formulations for the viscosity and thermal conductivity of water substance. J. Phys. Ref. Data 15(4):1291–1314.

SIAU, J. F. 1983. Chemical potential as a driving force for nonisothermal moisture movement in wood. A model for unsteady-state gas flow in the longitudinal direction in wood. Wood Sci. Technol. 17(2):101–105.

———. 1984. Transport process in wood. Springer-Verlag, New York, NY. 245 pp.

———. 1992. Nonisothermal diffusion model based on irreversible thermodynamics. Wood Sci. Technol. 26(5): 325–328.

———. 1995. Wood: Influence of moisture on physical properties. Dept. of Wood Sci. and Forest Prod. Virginia Polytechnic Institute and State University, Blacksburg, VA. 227 pp.

SKAAR, C. 1988. Wood-water relations. Springer-Verlag, New York, NY. 283 pp.

———, AND N. KURODA. 1985. Application of irreversible thermodynamics to moisture transport phenomena in wood. Pages 152–158 *in* Proc. North American Drying Symposium, Mississippi Forest Products Utilization Laboratory, Mississippi State Univ., MS.

STANISH, M. A., G. S. SCHAJER, AND F. KAYIHAN. 1986. A mathematical model of drying for hygroscopic porous media. AICHE J. 32(8):1301–1311.

ŚWIGOŃ, J. 1993. Some thermodynamic aspects of wood vacuum drying. Pages 35–44 *in* P. Trebula, ed. Vacuum Drying of Wood '93. High Tatras, Slovak Republic.

———, AND T. KURASIAK. 1995. Influence of vacuum on time of convective drying of wood. Pages 191–198 *in* P. Trebula, ed. Vacuum Drying of Wood '95. High Tatras, Slovak Republic.

TREMBLAY, C., A. CLOUTIER, AND Y. FORTIN. 1998. Determination of the effective water conductivity of red pine sapwood. Accepted for publication in Wood Sci. Technol.

WHITAKER, S. 1977. Simultaneous heat, mass and momentum transfer in porous media: A theory of drying. Pages 119–203 *in* J. P. Hartnett and T. F. Irvine Jr. eds. Advances in heat transfer, vol. 13, Academic Press, New York, NY.

———, AND W. T. H. CHOU. 1983. Drying of granular porous media. Theory and experiment. Drying Technol. 1(1):3–33.

NOTICE TO AUTHORS AND SUBSCRIBERS

Increased publication costs make it necessary for the Society to increase page charges and subscription prices for *Wood and Fiber Science* as follows: Effective with manuscripts received in July 1999 or later, page charges will be $90 per page for members of SWST and $110 for nonmembers. In the case of multiple authors, only one author need be a member for the member rate to apply. Changes in proof will be billed to the author at $3.00 per line. Effective with Volume 32(1) in January 2000, the subscription cost of the journal will be $125 per volume.

Robert L. Youngs, *Editor*